Effect of Gravity Gradient on Attitude Control of a Space Station

DONALD J. LISKA* AND WARD H. ZIMMERMAN*
The Boeing Company, Seattle, Wash.

A comprehensive analysis is made of the attitude control impulses required to totally counteract gravity-gradient torque on a sun-oriented, earth-orbiting space vehicle. The analytical approach divides the gravity-gradient torque into components according to significant frequencies. The analysis uses a unique orbit-referenced, "quasi-inertial" coordinate system into which the disturbance impulse vector is resolved. A long-period impulse component at twice orbit precession frequency appears along a coordinate axis in the orbit plane and perpendicular to the sun line-of-sight. Shorter-period components at twice orbital frequency appear along the other two coordinate axes. The short-period components can be controlled entirely with momentum exchange devices but the long-period component should be discharged with reaction jets. By fully utilizing the short-term storage capability of momentum exchange devices and applying combinations of controlled motions of the vehicle about its sun-oriented axis, the propellant consumed in overcoming the long-period disturbance is shown to be significantly reduced. The advantage of intentionally misaligning the vehicle axis from the sun line-of-sight is also shown.

Nomenclature

$\tilde{I}, \tilde{J}, \tilde{K}$	= local-vertical coordinate system
$\bar{I}, \bar{J}, \bar{K}$	= quasi-inertial coordinate system
$\tilde{i}, \tilde{j}, \tilde{k}$	= vehicle principal-axes coordinate system
A, B, C	= vehicle principal moments of inertia about $\tilde{i}, \tilde{j}, \tilde{k}$, respectively
$\bar{T}$	= gravity-gradient torque vector, ft-lb
$\bar{L}$	= gravity-induced impulse vector, ft-lb-sec
$\lvert\bar{L}\rvert$	= scalar magnitude of gravity-induced impulse vector, ft-lb-sec
$L_{\bar{I}, \bar{J}, \bar{K}}$	= impulse vector components along $\bar{I}, \bar{J}, \bar{K}$
l	= reaction-jet moment arm, ft
I_{sp}	= propellant specific impulse, sec
MED	= momentum exchange device
ACJ	= attitude-control jet
θ	= angle between vehicle $\tilde{k}$ axis and orbit plane
$\Delta\theta_e$	= allowable error angle between vehicle $\tilde{k}$ axis and sun line-of-sight (LOS)
θ_s	= optimum switching angle between constant-angle and constant-rate control laws
ϕ	= orbit position relative to $\bar{J}$ axis
$\dot{\phi}$	= orbital rate, rad/sec
β	= angle between $\bar{J}$ axis and vehicle $\tilde{i}$ axis (measured about $\tilde{k}$)
$\dot{\beta}$	= vehicle rotational rate (measured about $\tilde{k}$), rad/sec
ξ	= angle between autumn equinox and ecliptic node line
R_0	= orbital-radius magnitude to vehicle center of mass, ft
Q	= normalizing factor
γ	= orbit regression angle measured from ecliptic plane
ψ	= angle between sun LOS and ecliptic node line
i	= angle between ecliptic and orbital planes
α	= inclination of orbit to equatorial plane
i_e	= angle between $\bar{J}$ axis and ecliptic plane
GM	= gravitational constant of the earth

Introduction

DERIVATIONS of the torque produced by the gravitational gradient on an orbiting body have appeared in the literature on several occasions. Two classes of problems have received considerable attention: 1) the generalized motion of a body under the influence of the gravity torque alone when released from an arbitrary set of initial restraints,[1, 2] and 2) the application of the gravity torque as a medium of passive attitude or orientation control.[3] The increased interest in large orbiting stations and long-term missions has directed emphasis toward understanding the gravity gradient as a source of disturbance on an attitude-controlled vehicle. Of particular concern are the effects on sun- or inertially-oriented vehicles. The torque resulting from gravity gradient is proportional to the differences between the principal moments of inertia of a body. For sun- or inertially-oriented vehicles, a cumulative effect exists which is typically two orders of magnitude greater than the next largest disturbance (aerodynamics). In Ref. 4 the gravity torque on a sun-oriented vehicle was determined for a vehicle fixed in the ecliptic plane; in Ref 5 an analysis was carried out for a large disk-like space station.

The analysis presented in this paper is directed toward: 1) defining a rationale by which the vehicle attitude may be chosen to minimize the gravity-gradient effect, 2) defining the gravity-gradient effect in such a way that its relationship to vehicle configuration can be clearly described as an aid to design, and 3) introducing a unique coordinate system in order to provide a statement of the gravity-gradient torque, which significantly simplifies the calculation of its disturbance effect as a function of required control effort. The case of the rapidly spinning, sun-oriented vehicle is briefly discussed in terms of the gravity-gradient disturbance generated during rapid spin. In obtaining the fundamental torque equation, the vehicle is rigorously constrained to remain sun-oriented, thus requiring a perfect attitude-control system in order to isolate the gravity torque in terms of a specifically assigned attitude profile. Therefore, details of rigid body motion such as gyroscopic precession play no role in this analysis; it is merely assumed at the outset that the "perfect" control system performs the desired functions and that the vehicle provides an inertia distribution and attitude for determining the gravity torque, but enters into no relationships, which are rightly the domain of specific control system dynamics.

Gravity-Gradient Torque in Quasi-Inertial Coordinates

The derivation of the vector expression for the gravity-gradient torque in Ref. 1 treats the earth as a central force-field source and assumes the vehicle to be rigid. Even with these

Presented at the AIAA Space Station Symposium, Pasadena, Calif., April 15, 1964 (no preprint); received May 18, 1964; revision received February 5, 1965.

* Research Specialist, Space Vehicle Controls.

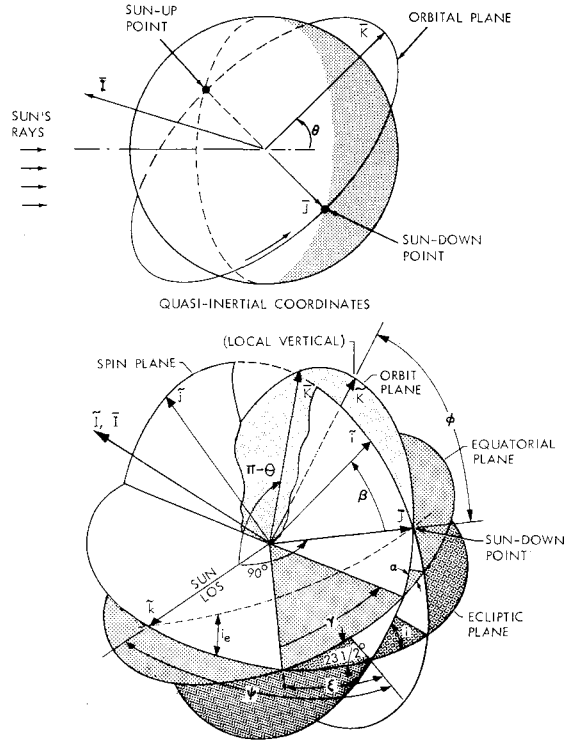

Fig. 1 Coordinate systems and transformation angles.

simplifications, the torque vector involves a series expansion of functions of the orbit radius vector. Neglect of higher order terms in this expansion is justified on the basis of order of magnitude of effect (10^{-6}), and the torque vector is reduced to a readily integrable form with only a small sacrifice in generality and precision. In Ref. 6, the resulting torque vector is further resolved onto a unique "quasi-inertial" set of orthogonal coordinates. It can be shown that

$$T = \{(3GM/R_0^3)[(\tilde{j}\cdot\bar{J})(\tilde{j}\cdot\bar{K})(A - B) + (\tilde{k}\cdot\bar{J})(\tilde{k}\cdot\bar{K})(A - C)]\bar{I}\} - (3GM/R_0^3)[(\tilde{j}\cdot\bar{I})(\tilde{j}\cdot\bar{K})(A - B) + (\tilde{k}\cdot\bar{I})(\tilde{k}\cdot\bar{K})(A - C)][(\tilde{J}\cdot\bar{J})\bar{J} + (\tilde{J}\cdot\bar{K})\bar{K}]\} \quad (1)$$

where $\tilde{j}$ and $\tilde{k}$ are vehicle coordinates, $\tilde{I}$, $\tilde{J}$, and $\tilde{K}$ are local vertical coordinates, and $\bar{I}$, $\bar{J}$, and $\bar{K}$ are "quasi-inertial" coordinates (Fig. 1). Note that one quasi-inertial axis $\bar{J}$ is in the orbit plane and is constrained to remain perpendicular to the sun LOS. In so doing, it must be directed along a line joining the points at which the orbit passes over the earth's shadow. Another axis $\bar{I}$ is perpendicular to the orbit plane and thereby coincident with $\tilde{I}$ in local-vertical coordinates.

Equation 1 can be geometrically expanded in terms of time-varying angles defining orbital motions. The body is assumed to be oriented with one principal axis, the $\tilde{k}$ axis, inertially oriented (for example, toward the sun), and is allowed freedom of rotation about that axis. Perfect attitude control is assumed, and the gravity torque is treated as a disturbance that does not perturb the motion of the vehicle. The reference planes and angles of motion are defined in Fig. 1. Solution of spherical triangles provides the scalar products of Eq. (1) as functions of the angles in Fig. 1.

$$(\tilde{j}\cdot\tilde{I}) = \cos\beta\cos\theta \qquad (\tilde{k}\cdot\tilde{I}) = \sin\theta$$
$$(\tilde{j}\cdot\tilde{J}) = -\sin\beta\sin\phi - \cos\beta\cos\phi\sin\theta$$
$$(\tilde{k}\cdot\tilde{J}) = \cos\phi\cos\theta$$
$$(\tilde{j}\cdot\tilde{K}) = -\sin\beta\cos\phi + \cos\beta\cos\phi\sin\theta$$
$$(\tilde{k}\cdot\tilde{K}) = -\sin\phi\cos\theta$$
$$(\tilde{J}\cdot\tilde{J}) = \sin\phi \qquad (\tilde{J}\cdot\tilde{K}) = -\cos\phi$$

Substituting into Eq. (1) gives the gravity-gradient torque equation in the quasi-inertial coordinate system:

$$\left.\begin{aligned}(2R_0^3/3GM)\bar{T} = {} & \sin2\phi\{[(A - B)(-\cos^2\beta\sin^2\theta + \sin^2\beta) - (A - C)\cos^2\theta]\}\bar{I} + [(A - B)\cos^2\beta\sin\theta\cos\theta - (A - C)\sin\theta\cos\theta]\bar{K} + \\ & \text{Short period} \\ & \sin2\theta\{-(A - B)\cos^2\beta\sin^2\phi + (A - C)\sin^2\phi\}\bar{J} + \\ & \text{Long period} \\ & \sin2\beta\{[(A - B)\cos2\phi\sin\theta]\bar{I} + [(A - B)\sin\phi\cos\phi\cos\theta]\bar{J} - [(A - B)\cos^2\phi\cos\theta]\bar{K}\} \\ & \text{Period dependent on } \beta\end{aligned}\right\} \quad (2)$$

In obtaining Eq. (2) it is assumed that the vehicle moves in a circular orbit and that the earth moves in a circular path about the sun. This preserves the most essential characteristics of the gravity-gradient torque without compounding its complexity. The choice of quasi-inertial coordinates was extremely important. These coordinates present the gravity-gradient torque as a set of three, very systematically behaved components along unit vectors. The three torque components may be grouped by terms according to frequency. The first grouping of terms in Eq. (2) involves components along $\bar{I}$ and $\bar{K}$; these are modulated at twice orbital frequency. Their frequency characteristic, as it affects the attitude control of the vehicle, is called "short period." The second grouping of terms contains only torque elements along the $\bar{J}$ axis; these are modulated at twice orbit precession frequency (modified by earth motion about the sun). Compared with the short-period terms, this is very low frequency and in general produces an "accumulation" of torque impulse over periods of several weeks. The last grouping of terms in Eq. (2) contains elements from along all of the three axes. These terms will be either short period or accumulating, depending upon the vehicle motion angle β about $\tilde{k}$.

Since β appears throughout Eq. (2), it can have a significant effect on the magnitude and sense of each torque component. The vehicle $\tilde{k}$ axis is the one assumed to be sun- or inertially-oriented; therefore, one can consider that β may be established to modify the effect of the gravity gradient on the vehicle. Several control laws were developed to exploit this characteristic of β. The short-period terms of Eq. (2) are likely candidates for control with momentum exchange devices or, in the case of a spinning vehicle where $\beta \gg \dot{\phi}$, will produce negligible perturbations of vehicle attitude. The cumulative torque, however, generally must be controlled by external reaction jets.

Attitude Control Laws

In studies conducted on large, rod-shaped space stations with fixed solar panels, orbiting at altitudes above 250 miles, it was found that the gravity-gradient torque disturbances were two orders of magnitude greater than the next largest disturbance (aerodynamics). Several "gravity-gradient control laws" were therefore devised; they were based on manipulation of the vehicle attitude about the sun LOS to maintain an advantageous attitude relative to local vertical while fulfilling the sun-orientation requirements. These laws were called "exact horizontal control," "constant-angle control," "constant-rate control," and "sun-error." They are based on fundamental motions or attitudes of the vehicle and, in some cases, can be used in combination to increase their effectiveness in reducing the gravity-gradient disturbance. These laws basically belong to the "nonspinning" operational mode of the vehicle since the nominal angular rate does not exceed orbital rate. The "spinning" mode of operation, on the other hand, implies nominal angular rates considerably greater than orbital rate and poses a distinctly different class of control problem involving a predominance of precession and nutation factors.

Nonspinning Mode

Exact horizontal control

The requirement that the fixed solar panel axis be pointed toward the sun prevents alignment of the axis of minimum inertia with local vertical, which would both stabilize the vehicle and eliminate the gravity torque. It is possible to maintain one principal axis exactly horizontal, however, and still track the sun with the solar panel axis if active control of rotational attitude is applied about the sun-pointed axis. A precisely horizontal attitude of the minimum inertia axis results in a large reduction of gravity torque (indeed, for a symmetrical rod-shaped vehicle, the torque vanishes) although this attitude is only marginally stable in the uncontrolled sense. The modulation of rotational rate about the sun LOS required by this method offsets its intent, however, because of excessive propellant requirements at small values of θ. Horizontal control is only desirable at large values of θ where it merges with rotation at orbital rate for $\theta = 90°$. It is furthermore apparent that at $\theta = 0°$ (orbit plane and sun LOS coincident) exact horizontal control is accomplished by stabilizing the vehicle in "quasi-inertial" coordinates, that is, reducing its rotational rate relative to $\bar{I}$, $\bar{J}$, and $\bar{K}$ to zero. These facts lead to the generation of two additional laws, one good for small θ and the other for large θ. They are the constant-angle and constant-rate control laws, in both of which the axis of maximum inertia should be oriented toward the sun for good control.

The constant-angle control law

This law is initiated at either of the two points in the orbit plane where the vehicle $\tilde{k}$ axis (in the case of a sun-oriented vehicle, this is also the sun LOS) is perpendicular to local vertical. The initial conditions require that the vehicle be rotated about $\tilde{k}$ until $\tilde{i}$ is horizontal. This inertial attitude is then held for 180° of orbit angle and is reset if necessary to comply with the progression of the $\bar{J}$ axis (as defined by the angle i_e in Fig. 1). The gravity torque [Eq. (2)] is reduced by substituting $\beta = \pi/2$, and the gravity-gradient torque for constant-angle control is

$$(2R_0^3/3GM)\bar{T} = \{\sin 2\phi[(A - B) - (A - C) \times \cos^2\theta]\bar{I}\}\{+ \sin 2\theta[(A - C)\sin^2\phi]\bar{J}\} + \{\sin 2\phi[-(A - C)\sin\theta\cos\theta]\bar{K}\} \quad (3)$$

It will be noted that the $\bar{J}$ component of Eq. (3) is cumulative in accordance with the definition given in deriving Eq. (2) and that this component goes to zero as θ approaches zero and is maximum when $\theta = 45°$. For $\theta = 0$, the $\bar{K}$ component is zero, and the other short-period torque component along $\bar{I}$ is minimized in rod-like vehicles ($A < B \leq C$) by orienting the axis of minimum inertia along $\bar{I}$. Thus, *when θ is small, the gravity torque will be very small* when following the constant-angle control law, even for exact sun orientation.

The maximum torque amplitude about the $\bar{I}$ axis occurs for $\theta = 90°$. In this case the quasi-inertial $\bar{I}$ axis and the vehicle $\tilde{k}$ axis are colinear. In local-vertical coordinates, the vehicle appears to rotate in the orbit plane through local vertical. If, as has been assumed, $A < B \leq C$, this condition produces the maximum short-period torque amplitudes about $\bar{I}$. The maximum amplitude for the $\bar{K}$ component occurs when $\theta = \phi = 45°$ since, under this condition, the deviation of the $\tilde{i}$ axis out of the orbit plane is most nearly 45°.

It has been shown that the constant-angle control law is most applicable when θ is small. The magnitude of all three torque components can be minimized in a rod-like vehicle.

The constant-rate control law

As in the constant-angle control law, this law is initiated at the points where the vehicle $\tilde{k}$ axis is perpendicular to local vertical. Here, however, after rotating about $\tilde{k}$ until the $\tilde{i}$ axis is in the horizontal plane, the vehicle is given an angular rate about $\tilde{k}$ equal to orbital rate and in the same sense as the projection of $\dot{\phi}$ on to the sun LOS. The gravity torque [Eq. (2)] is modified by substituting $\beta = \phi + \pi/2$, and the gravity-gradient torque equation for constant-rate control is

$$(2R_0^3/3GM)\bar{T} = \{\sin 2\phi[(A - B)(-\sin^2\phi\sin^2\theta + \cos^2\phi - \cos 2\phi\sin\theta) - (A - C)\cos^2\theta]\bar{I}\} + \{[-(A - B)(\sin 2\theta\sin^4\phi + \tfrac{1}{2}\sin^2 2\phi\cos\theta) + (A - C)\sin 2\theta\sin^2\phi]\bar{J}\} + \{\sin 2\phi[(A - B) \times (\sin^2\phi\sin\theta\cos\theta + \cos^2\phi\cos\theta) - (A - C)\sin\theta\cos\theta]\bar{K}\} \quad (4)$$

Note that the cumulative component along $\bar{J}$ does not go to zero as θ approaches zero. The maximum short-period torque amplitudes are not readily found as were those for the constant-angle law since they are far more complex functions of ϕ, θ, and the vehicle configuration. The short-period torques are zero, however, at the quarter orbit points ($\phi = 0°$, 90°, and 180°, etc.). As θ approaches 90°, Eq. 4 reduces to zero since two vehicle axes ($\tilde{i}$ and $\tilde{k}$) are constrained to lie in the horizontal plane, thus making the $\tilde{j}$ axis vertical. Under this condition, no gravity torque is possible. Thus, the constant-rate control law is most effective for large θ.

The sun-error law

Basically, this law makes use of any angular tolerances allowed in pointing the solar panels toward the sun to modify the ranges of θ during which constant-angle and constant-rate control are applied. As such, it is not a uniquely different control law. The error angle is determined by the tolerances on the solar collector. Flat collectors have a fairly wide angular tolerance about which collected power does not drop off significantly. A study was made showing that the power loss with a 13° sun error was acceptable for flat collectors proposed by Boeing for the Manned Orbital Research Laboratory (MORL).

The allowable sun-orientation error is used by maintaining the vehicle $\tilde{k}$ axis (the sun-pointing axis) in the orbit plane until the maximum pointing error $\Delta\theta_e$ is reached. In effect, this extends the time over which perfect constant-angle control can be used (zero accumulating impulse). The vehicle is then held at the $\Delta\theta_e$ limit under constant-angle control until the optimum switchover angle is reached and is then put into constant-rate control. Now the $\tilde{k}$ axis is shifted so that the plane of vehicle rotation about $\tilde{k}$ is as near the orbit plane as $\Delta\theta_e$ will allow. This serves to increase the level of θ for constant-rate control to as large a value as possible. As was pointed out in Eq. (4), the larger θ becomes, the less significant is the accumulating $\bar{J}$ torque component and the less propellant is required to control it. The over-all effectiveness of $\Delta\theta_e$ on reducing impulse requirements increases as the allowable $\Delta\theta_e$ increases. A sample calculation[6] for one MORL configuration showed an average propellant saving per orbit of over 60% when an allowable sun error of 13° was fully utilized.

Spinning Mode

In the spinning mode, the vehicle angular rate about the sun LOS may be considerably greater than orbital rate, e.g., $\dot{\beta} > 100\dot{\phi}$. The rapidly spinning vehicle, therefore, is not subject to selective orientation to reduce the gravity-gradient torque, and unless counteracted, the cumulative component along $\bar{J}$ will cause the spin axis to precess. The short-period components of torque may generally be neglected because of their low integrated impulse content. If rapid spin is only intermittently required, the best times to apply it are when θ is 0° or 90°. Under these conditions the vehicle spin plane is either horizontal or vertical, and cumulative disturbance effects are minimized.

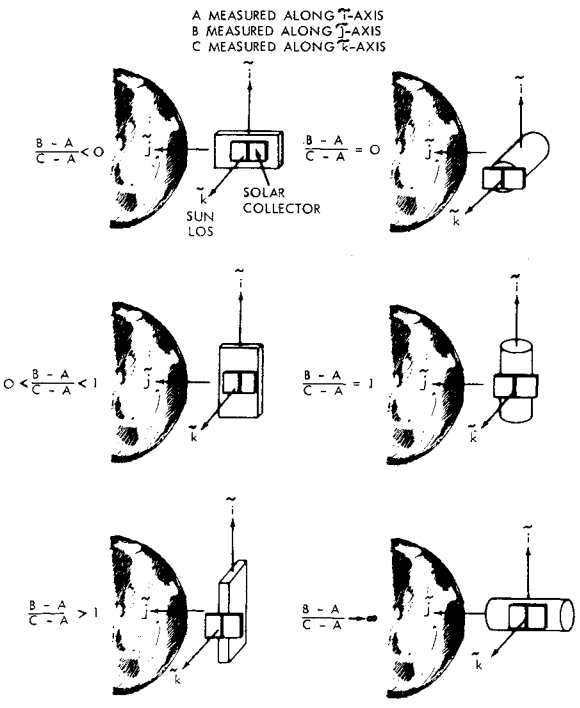

Fig. 2 Generalized configurations.

Gravity-Gradient Impulses and Design Curves

A useful result that came out of this study is the parametric presentation of the short-period and accumulating-disturbance impulses imposed on the vehicle by the gravity torque. These parametric data allow the size and capacity of the control system, of whatever type, to be estimated. The choice of the best type of control system also becomes more straightforward. The gravity-gradient impulses are obtained by integrating the torque components for the various motions included under both nonspinning and spinning operations. The resulting impulses are plotted parametrically where the results are thought to be useful in spacecraft design. A circular orbit is assumed in all of the cases.

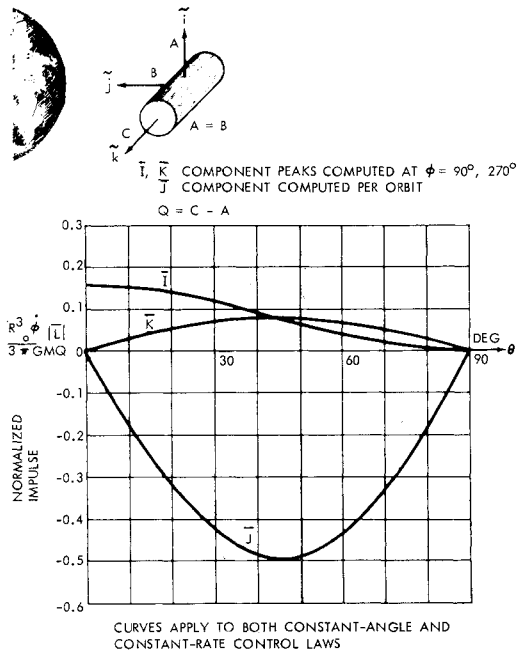

Fig. 3 Disturbance impulse on rod-like vehicle.

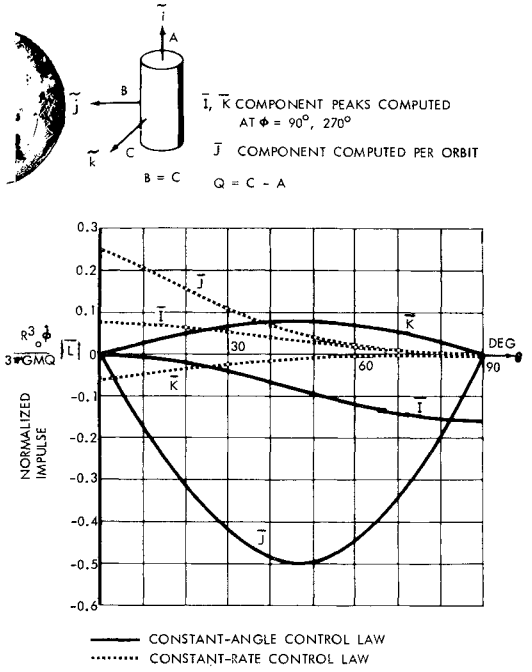

Fig. 4 Disturbance impulse on rod-like vehicle.

Nonspinning Mode

Exact horizontal control has disadvantages, which overrule its ability to eliminate the gravity-gradient torque, but it points the way to the very useful constant-angle and constant-rate control laws. Since these laws serve opposite ends of the range of θ, they can be used as a guide in selecting preferred configurations and orientations of the nonspinning vehicle. By integrating Eqs. (3) and (4) with respect to orbit position, the disturbance impulse components can be found.

Constant-angle control, accumulating disturbance

Integrating the $\bar{J}$ torque component of Eq. (3) over one complete orbit results in the accumulated-disturbance impulse per orbital period

$$\frac{R_0^3\dot{\phi}}{3\pi GM(C-A)}\bar{L} = -\frac{1}{2}\sin 2\theta\,\bar{J} \qquad (5)$$

accumulation per orbit

This integration is justified since θ does not change significantly during an orbital period.

Constant-angle control, short-period disturbance

To provide information useful in sizing momentum exchange devices with which to control the short-period torques, it is necessary to determine the *maximum*-disturbance impulse to which these devices will be exposed. The fundamental frequency of the oscillating impulse is at twice orbital frequency as is the gravity torque itself. Because of the complex nature of the torque, however, the peak impulse does not occur precisely at the first and last quarter-orbit points. The actual maximum is tedious to determine, but sufficient accuracy is obtained by assuming the quarter-orbit-point impulse to be an adequate indication of required control capacity. Thus, the $\bar{I}$ and $\bar{K}$ components of Eq. (3) are integrated at constant θ, whereas ϕ varies from 0° to 90°.

$$\frac{2R_0^3\dot{\phi}}{3GM(C-A)}\bar{L} = \left[\cos^2\theta - \left(\frac{B-A}{C-A}\right)\right]\bar{I} + \frac{1}{2}\sin 2\theta\bar{K} \qquad (6)$$

peaks at ϕ = 90°, 270°

Constant-rate control, accumulating disturbance

Integrating the $\bar{J}$ torque component of Eq. (4) over one orbit results in the gravity-induced disturbance impulse accumulated per orbital period using constant-rate control

$$\frac{R_0^3\dot{\phi}}{3\pi GM(C-A)}\bar{L} = \left[\left(\frac{B-A}{C-A}\right)\left(\frac{3}{8}\sin 2\theta + \frac{1}{4}\cos\theta\right) - \frac{1}{2}\sin 2\theta\right]\bar{J} \quad (7)$$

accumulation per orbit

Constant-rate control, short-period disturbance

In the same manner as for constant-angle control, this disturbance is found by integrating the short-period torque components of Eq. (4) over a quarter orbit

$$\frac{2R_0^3\dot{\phi}}{3GM(C-A)}\bar{L} = \cos^2\theta\left[1 - \frac{1}{2}\left(\frac{B-A}{C-A}\right)\right]\bar{I} + \cos\theta\left\{\sin\theta\left[1 - \frac{1}{2}\left(\frac{B-A}{C-A}\right)\right] - \frac{1}{2}\left(\frac{B-A}{C-A}\right)\right\}\bar{K} \quad (8)$$

peaks at $\phi = 90°, 270°$

Impulse Curves for Symmetrical Vehicles

By treating the vehicle in a general manner, a complete set of orientations and configurations can be constructed as in Fig. 2. It can be shown that certain of these choices are preferred over others on the basis of the relative magnitudes of the oscillating- and accumulating-disturbance impulses. Although any vehicle configuration can be analyzed, the ideal rod-like vehicles (equal inertias about two axes) allow the impulses [Eqs. (5–8)] to be plotted in their most elementary and revealing forms. This is done in Figs. 3–5 for three orthogonal orientations of the same vehicle. The vehicle $\tilde{k}$ axis is directed toward the sun, and the $\tilde{j}$ axis is directed along local vertical at the sun-up and sun-down points. The normalizing factor Q is either $(A\text{-}B)$ or $(C\text{-}A)$ depending upon the orientation. Note, however, that $(A\text{-}B)$ in Fig. 6 is equivalent to $(C\text{-}A)$ in Figs. 3 and 4. This makes the total normalizing factor identical in all of the three cases and allows Figs. 3–5 to be directly compared on a numerical basis. Note also that each orientation can be treated as a disk or thin rod with no exclusions in between but that this significance of Q must be applied equally in all of the cases to retain the desired comparative feature.

Figure 3 reveals the major disadvantage of a disk- or rod-like vehicle with its axis of circular symmetry pointed to the sun. Since spin attitude about $\tilde{k}$ is ambiguous, the same disturbance impulse is generated for both the constant-angle and constant-rate control laws. Furthermore, the cumulative impulse along the quasi-inertial $\bar{J}$ axis is very large for the widely different A and C. This orientation is considered poor and should be discarded in favor of the orientations shown in Figs. 4 and 5. The gravity-gradient control laws are quite effective in the Fig. 4 orientation. Transfer between constant-angle control and constant-rate control should occur at $\theta \simeq 11°$, and all of the disturbance impulse components switch accordingly. Figure 5 reveals an orientation in which there is no accumulating-disturbance impulse for $A = C$ if constant-angle control is used. The choice here is very clear-cut in that constant-rate control is decidedly undesirable with its large cumulative and oscillating impulse components.

The important choice then lies between the use of the orientations of Figs. 4 and 5. Many factors may affect this choice, and the mission requirements may specify it. Disregarding the mission, however, the two factors that pointedly decide the choice are the actual difference between the two largest moments of inertia and the use of sun-error control, which is completely ineffective when the vehicle is oriented

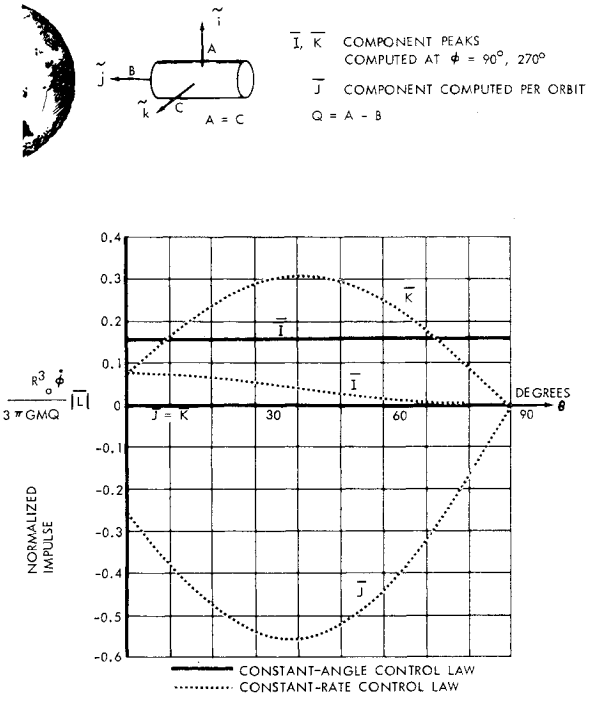

Fig. 5 Disturbance impulse on rod-like vehicle.

as in Fig. 5, since rotational attitude about the $\tilde{j}$ axis is ambiguous in mitigating the disturbance torques. In Fig. 4, however, sun-error control is quite effective, as is established in Ref. 6. Therefore, if the sun-error control is applied, and if a significant difference exists between the two largest moments of inertia of the vehicle, the orientation given in Fig. 4 is preferred.

A wide range of nonsymmetrical vehicles is treated in design curves in Ref. 6. Generation of these curves is not difficult and is based on the application of Eqs. (5–8).

Spinning Mode

By imposing certain additional restrictions, it is possible to integrate Eq. (2) for a rapidly spinning vehicle. If $\dot{\beta} \gg \dot{\phi} \gg \dot{\theta}$, then ϕ and θ can be considered constant over a single spin cycle. This is reasonable if $\dot{\beta} > 100\ \dot{\phi}$, e.g., since for earth orbits, $\dot{\phi} \gg 100\dot{\theta}$. If an even number of spin cycles are assumed per orbit, the period-dependent terms of Eq. (2)

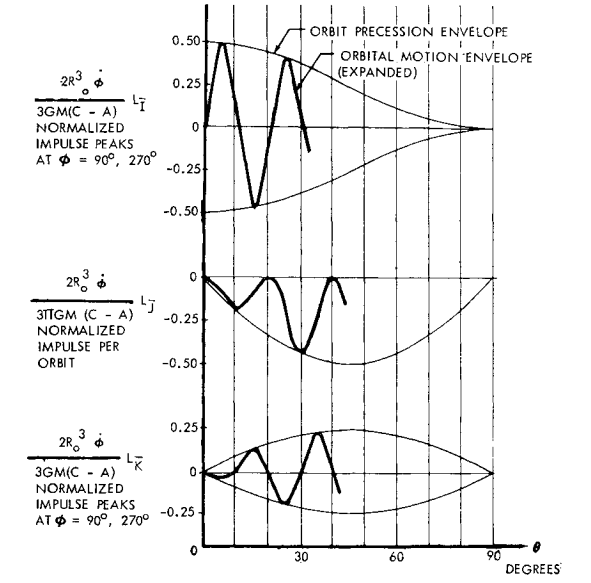

Fig. 6 Design application of constant-angle and constant-rate control.

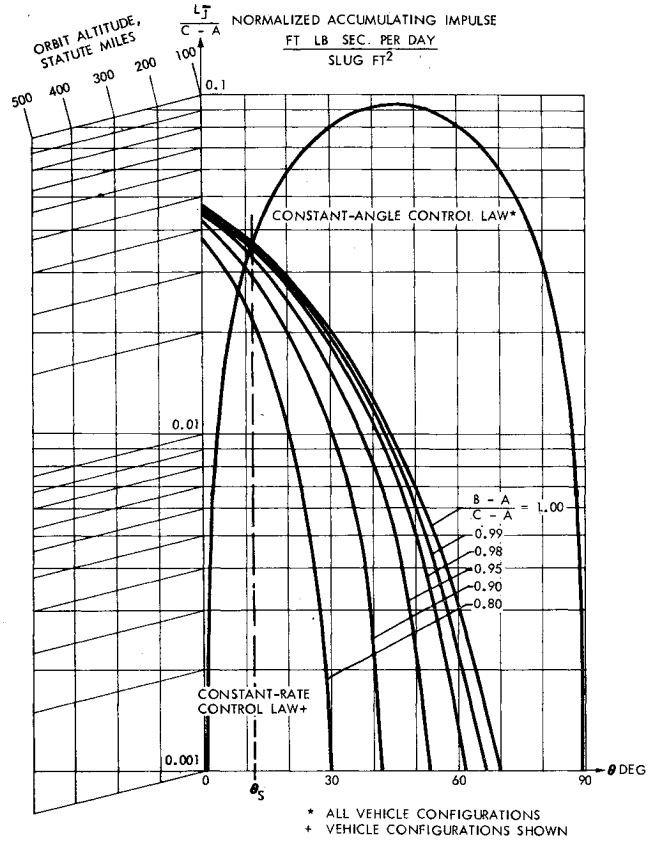

Fig. 7 Impulse envelope for rapidly spinning vehicle.

integrate to zero. The disturbance impulse equation can therefore be derived as

$$\frac{2R_0^3\dot{\phi}}{3GM(C-A)}\bar{L} = \underbrace{\left\{\left[1-\frac{1}{2}\left(\frac{B-A}{C-A}\right)\right]\cos^2\theta\right\}\bar{I}}_{\text{peaks at } \phi = 90°,\ 270°} - \underbrace{\pi\left\{\left[1-\frac{1}{2}\left(\frac{B-A}{C-A}\right)\right]\sin 2\theta\right\}\bar{J}}_{\text{accumulation per orbit}} + \underbrace{\frac{1}{2}\left\{\left[1-\frac{1}{2}\left(\frac{B-A}{C-A}\right)\right]\sin 2\theta\right\}\bar{K}}_{\text{peaks at } \phi = 90°,\ 270°}$$

These torque components are plotted in Fig. 6. It is interesting to compare the $\bar{J}$ components for rod- and disk-shaped vehicles where the disk-shaped vehicle has its axis of symmetry toward the sun. The inertia ratios are $[(B-A)/(C-A)] = 1$ and 0, respectively, in this case, and the $\bar{J}$ components become

$$[2R_0^3\dot{\phi}/3GM(C-A)]\,\bar{L} = -(\pi/2)\sin 2\theta\bar{J}$$

and

$$= -\pi\sin 2\theta\bar{J}$$

for a rapidly spinning rod and for a disk, respectively. Thus it is seen that rapid spin has an "inertia-averaging" effect on the rod-shaped vehicle such that the accumulating impulse is half that for a disk.

Parametric and Trade Studies

The preceding analyses were applied to nonspinning MORL configurations studied at Boeing. These were rigid, elongated vehicles with approximately equal maximum principal inertias ($A \ll B \backsimeq C$). Fuel estimates for various missions were based on orientating the vehicle as in Fig. 4 and using constant-angle, constant-rate, and sun-error attitude control.

Two useful sets of data were obtained. The first is the parametric study described in Fig. 7, which clearly shows the switchover angle between constant-angle and constant-rate control. The usefulness of Fig. 7 is extended by using the log scale in order to provide a linear adjustment for orbital radius R_0. Several vehicle configurations are shown for constant-rate control. The curve given for the constant-angle control is valid for all of the vehicles. This is because Eq. (5) shows that the constant-angle accumulating impulse is independent of the vehicle B inertia. Combined with the time history of θ for a given mission, Fig. 7 represents a powerful descriptive tool to aid in control system synthesis and fundamental trade studies. The equations necessary to solve for θ may be found readily from Fig. 1 by allowing for earth motion about the sun as well as precession of the orbit plane about the earth's polar axis. They are then used to provide θ distribution data for any initial conditions.

The other revealing set of data is given by study of Fig. 8, which was generated by assuming a symmetrical vehicle ($A \ll B = C$). In this manner, the trade study can be calculated for a single vehicle and can be linearly extrapolated for any vehicle on the same mission for which the equality of inertias is valid. The combined MED-ACJ system operates on the principle that the oscillating-disturbance impulses are completely controlled by the MED's, which also store the accumulating impulse for half-orbit periods. At the half-orbit points ($\phi = 0°$ and 180°), the ACJ's are provided with their longest moment arms about the $\bar{J}$ axis and require the least MED desaturation propellant.

For some of the space stations recently studied at Boeing, the parameter of Fig. 8 was about 150. For vehicles of this size, the propellant weight difference between the all-ACJ and combined MED-ACJ systems is so large that the fixed weight of the attitude-control system does not significantly affect the trade results for long-duration missions. Subsequent trade studies, which included the fixed weights as well as the weight of the control system expendables, have indicated that the integrated MED-ACJ system has a weight advantage for mission times beyond about 14 days, assuming continuous control is required.

The additional savings realized by using a 13-deg sun-pointing error is also shown in Fig. 8. Thus, by fully utiliz-

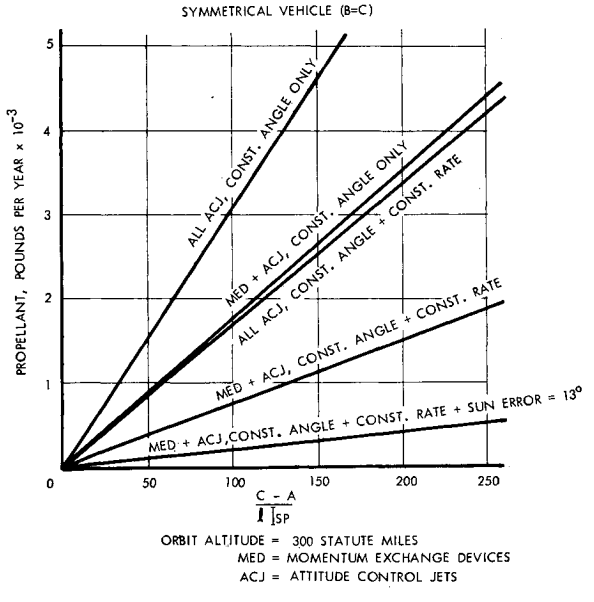

Fig. 8 Comparison of propellant weight affected by choice of control laws and control systems.

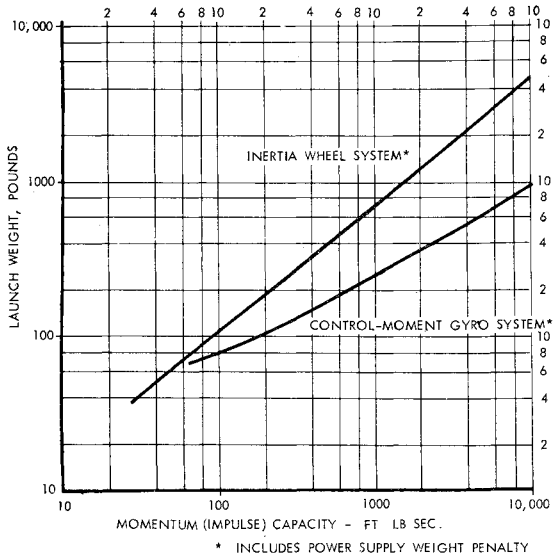

Fig. 9 Momentum exchange trade data.

ing MED's in an integrated attitude-control system, applying constant-angle and constant-rate control in combination, and using sun-pointing error, a total yearly fuel saving of 94% was realized over all ACJ constant-angle control only.

It remains to decide which MED is lightest and draws the least electrical power. In sizing the MED's it must be recognized that the cumulative gravity-gradient impulse is quasi-inertial along $\bar{J}$ and therefore must be shared between the vehicle $\bar{i}$ and $\bar{j}$ body axes when following the constant-rate control law. This interaxis coupling manifests itself as an *alternating* impulse with ever-increasing amplitude. Thus, inertia wheels will undergo alternations in speed, and (CMG) gimbal angles will alternate. Eventually, excessive wheel speed or gimbal angle will necessitate desaturation with the ACJ's. Note that these considerations do not apply to the rapidly spinning vehicle in which the MED's would not be used for gravity-gradient control, but rather for coning control and nutation damping. To control the cumulative gravity-gradient disturbance, momentum must be transferred from the MED's onto the $\bar{i}$ and $\bar{j}$ body axes, thus requiring two inertia wheels or two degrees of CMG freedom. The electrical power required to drive these devices, as well as the fixed hardware weights, are compared for a typical four-man space station of the MORL size in Fig. 9.

Conclusions

The gravity-gradient torque on a sun-oriented, orbiting body can be expressed in terms of three well-behaved vector components, which include both short-period and cumulative torques. To reduce the magnitude of the resulting gravity-induced disturbance impulse, two useful gravity-gradient control laws have been developed: the constant-angle and the constant-rate control laws. Related to these, a sun-error law is described which can be applied in conjunction with constant-angle and constant-rate control to further reduce the level of disturbance. The coordinate axes chosen to define the three gravity-torque vector components are termed quasi-inertial since they are fixed in the orbit plane and only move slowly in space because of precession of the orbit and earth motion about the sun.

The short-period torque impulses can be controlled by momentum exchange devices, but the cumulative components may be so controlled for a limited time only and must eventually be discharged with reaction jets. The optimum attitude-control system, therefore, uses a combination of momentum exchange devices and reaction jets, as well as applying constant-angle and constant-rate control along with the related sun-error law. With this system, the control authority about the two body axes perpendicular to the nominal sun LOS must be equal, and the control logic intermittently operates the reaction jets to discharge the accumulated-disturbance impulse about a quasi-inertial axis in the orbit plane. The control system for the nominally sun-pointed axis is required to control only an oscillating torque. Using this combination of control laws and combinations of ACJ's and MED's, sample calculations of propellant expenditure for a rod-like vehicle indicate a realizable saving as high as 94% a year over straight reaction jets with only constant-angle control (vehicle fixed in quasi-inertial coordinates). Vehicle configuration is a critical factor, which complicates the impulse calculations for shapes other than rods or disks. In general, the axis of maximum inertia should be the one which is solar-oriented.

References

[1] Nidey, R. A., "Gravitational torque on a satellite of arbitrary shape," ARS J. **30**, 203–204 (1960).

[2] Doolin, B. F., "Gravity torque on an orbiting vehicle," NASA TND-70 (1959).

[3] Roberson, R. E., "Attitude control of a satellite vehicle—An outline of the problems," IAC Eighth International Conference of Astronautics, International Astronautical Federation, Barcelona, Spain, pp. 317–339 (October 7–12, 1957).

[4] Hultquist, P. F., "Gravitational torque impulse on a stabilized vehicle," ARS J. **31**, 1506–1509 (1961).

[5] Schalkowski, S. and Cooley, W. C., "Gravity gradient torques on a sun-oriented space station," NASA TR 001 (December 1963).

[6] Liska, D. J. and Zimmerman, W. H., "Effect of gravity gradient on attitude control of a space station," unlimited Boeing Doc. D2-23348 (June 1964).